A New Elongation Function for Modelling Long Arcs in Open Air

G. Preston, M. Popov, Z.M. Radojević, V. Terzija.

***Abstract*— In this paper the behaviour of long electrical arcs in open air is investigated. An arc was induced and recorded in the high power test laboratory at FGH-Mannheim, Germany. The recorded data was then analysed to extract the features of the arc and used to derive a new quasi-dynamic arc model, including the elongation of the arc and the effects of random noise. The new arc model is a current dependent voltage source. It gives a non-linearly elongating distorted rectangular voltage, which is characteristic of long arcs in open air. Due to their distorted rectangular voltage waveform, fault arcs are known to be a significant source of harmonics that distort other voltages and currents on the power system, so an arc model must also accurately represent this aspect of the arc. The arc model was simulated using the ATP-EMTP software package and the time domain and spectral domain features of the simulated arc are compared with those of the real arc.**

***Index Terms*— Long arc in open air, arc length, laboratory testing, EMTP, modelling, simulation, distortions, spectral analysis.**

I. Introduction

LONG arcs in open air often occur during faults on electrical power systems. The length of the arc is influenced by factors such as the arc's supply current, the magnetic forces acting on the arc column caused by the supply current, the plasma of the arc, and the wind speed and atmospheric conditions surrounding the arc; this makes modelling the arc a particularly complicated matter. Electrical arcs are purely resistive and therefore the length of the arc has a significant influence on the arc voltage – the arc voltage increases proportionally to the arc length. The length of an arc in open air increases non-linearly throughout its duration and is subject to random noise.

The phenomenon of electrical arcs has attracted much research for over a century and many different arc models have been derived. The most popular and most accurate means of modelling dynamic AC arcs is through the theory of thermal equilibrium and energy balance. The earliest examples of this theory are given in [1] and [2]. A model of short arcs in circuit breakers was developed in [3]. The arc models presented in [4] and [5] have been proven to model long arcs in open air accurately, but they are highly complex and may be too burdensome to use in some areas of power engineering where a simple yet accurate arc model is required – such as defining the equivalent stationary arc resistance. A new formula for arc resistance was derived in [6] by using instantaneous values of the arc voltage and current and a static arc model. New numerical algorithms for fault location, fault analysis and smart autoreclosure based on the static arc model from [6] were published in [7]-[9].

Accurately modelling arcing faults helps engineers to gain a good comprehension of how arcing faults interact with the rest of the power system for transient process analysis and helps them to efficiently design power system protection schemes. Currently, several commercial software packages are available that can be used to simulate arcing faults [10]-[12].

The Electromagnetic Transients Program (EMTP) [10], [11] was developed to help power systems engineers with their studies into transient processes. The program was designed to allow the analysis of short circuit faults, load flow problems, and transient conditions. It can be used to simulate power system networks consisting of various components, and works by solving the algebraic and differential equations associated with the various connections of those components.

Early experimental studies into the behaviour of long arcs in open air are given in [13] and [14]; these studies are limited by the technology available at that time. Modern transient recorders with fast 16-bit A/D converters give more reliable field and laboratory test results; such technology was used to record the laboratory induced arc for this paper.

A series of investigations were undertaken into real arcs in the high power test laboratory FGH-Mannheim, Germany. The features of the laboratory arc are used to confirm the performance of the new arc model. The new quasi-dynamic arc model, including an elongation function and random noise, is derived, and the time and the spectral domain features of the simulated arc are presented and compared with those of the real arc.

II. High Power Laboratory Experiments

The physical nature of long arcs in open air and their variations in length were investigated in a series of experiments at the high power test laboratory FGH-Mannheim, Germany. The line terminal voltage, $u(t)$, arc current, $i(t)$ and arc voltage, $u_a(t)$, were recorded in digital format – all data was digitized with a sampling frequency of 0.16 MHz. The arc

G. Preston and V. Terzija are with The University of Manchester, UK, (e-mail: g.preston@student.manchester.ac.uk, terzija@ieee.org).

M. Popov is with the Delft University of Technology, The Netherlands, (e-mail: M.Popov@ieee.org).

Z. M. Radojević is with The Sungkyunkwan University, Suwon, Korea, (e-mail: radojevic@ieee.org).

Paper submitted to the International Conference on Power Systems Transients (IPST2011) in Delft, The Netherlands, June 14th-17th, 2011.

was induced by melting a fuse wire between two electrodes in a vertical insulator chain when switch S was closed. The distance between the electrodes was varied over the range of 170 – 200 cm. On inception ($t_i \approx 0.055$ s), the arc's length and voltage were immediately determined by the distance between the electrodes, but, as a 5 kA arc current flowed, significant arc elongation with corresponding increases in the arc voltage were observed over the arc's duration.

The recorded line terminal voltage $u(t)$ is presented in Fig. 1 and the recorded arc voltage $u_a(t)$ and arc current $i_a(t)$, are shown in Fig. 2. From Fig. 2, it can be seen that the arc voltage and current are directly in phase (confirming the arc's resistive nature) the arc length increases non-linearly, and the arc voltage is affected by random noise. Also, the non-linearity of the arc produces high frequency components that distort the arc voltage waveform into a distorted rectangular shape. However, that non-linearity has no effect on the arc current, which retains a sinusoidal waveform throughout. As the arc length increases, the resistance of the arc increases, leading to a slight decrease in the amplitude of the arc current; otherwise, the arc current is determined by the supplying network voltage, which is much larger than the arc voltage.

The arc voltage amplitude is proportional to the length of the arc. The two are related by the arc voltage gradient E_a, which has been found to be between 10-20 V/cm for arcs over a range of currents from 0.1-20 kA [13], [15], [16]. In [13] it was shown that there is a voltage drop at the electrodes of around 20-40 V, independent of the arc length. So, for long high voltage arcs, the total arc voltage appears almost entirely across the arc column, meaning that the voltage drop at the electrodes can be neglected.

In Fig. 3 the *u-i* characteristics of the recorded arc are shown. The characteristics are obviously random and time-varying; they show the non-linear nature of the arc, caused by the dynamic changes in the arc length.

As the arc is a non-linear element, it is a source of harmonics that cause distortions to the other currents and voltages on the network, including the line terminal currents and voltages. The level of the harmonic distortion is dependent upon the network topology and parameters, the arc voltage magnitude and the location of the arcing fault on the network – the level of distortion in a signal is proportional to the signal's proximity to the fault. The level of harmonic distortion in a signal is calculated using the total harmonic distortion factor, *THD*, as follows:

$$THD = \frac{100}{X_1}\sqrt{\sum_{h=2}^{M} X_h^2}\ \% \qquad (1)$$

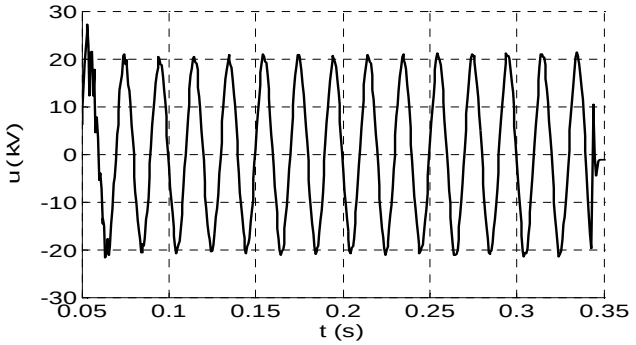

Fig. 1: Recorded line terminal voltage *u(t)*.

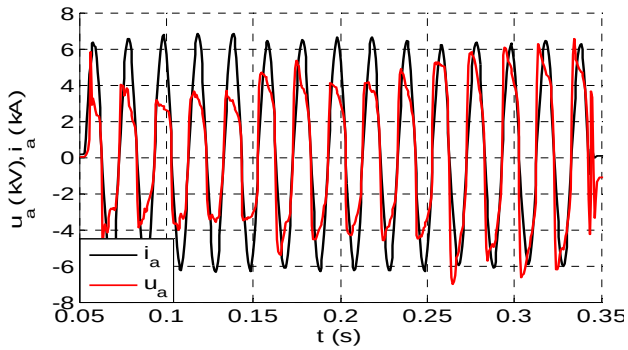

Fig. 2: Recorded arc voltage (red) and current (black).

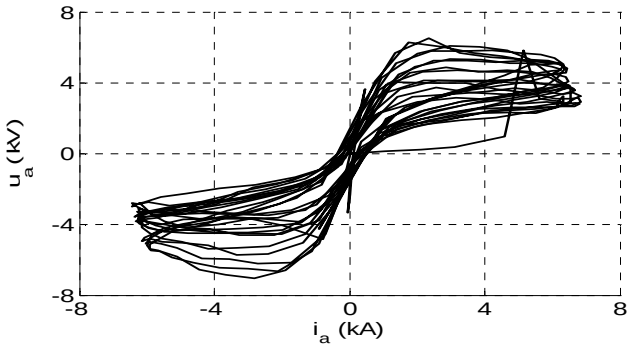

Fig. 3: Arc *u-i* characteristics.

III. Modelling of Long Arcs in Free Air

A. Arc Modelling.

The modelling of long arcs in free air has attracted much research attention in the past. Using the theory of thermal equilibrium and energy balance, the Arc voltage can be expressed using a non-linear differential equation [1], [2], [15], with the general form:

$$\frac{dg_a}{dt} = f(g_a, u_a, i_a, \Pi, t) \qquad (2)$$

The set of unknown parameters represented by Π must be estimated from test data from real arcs. Research has shown that Cassie's model [1] is suitable for heavy current arcs, whereas Mayr's model [2] is suitable for low current arcs – especially around the current zero-crossing.

Here a new static arc voltage model that accurately represents the effects of the arc elongation, as discussed in Section III, is presented. The new model is highly suited to arc simulation and implementation in the modern computer relaying numerical algorithms [7]-[9], and it was developed by observing the relationship between the arc voltage and arc current waveforms.

In Fig. 2 it was noted that the arc voltage waveform takes a distorted rectangular shape and is directly in phase with the arc current. Thus, the arc voltage can be modelled through the following non-linear equation [18], [19]:

$$u_{a0}(t)=\left(U_a+U_b\frac{I_0}{i_b(t)}+R_\delta\left|i_b(t)\right|\right)\ \mathrm{sgn}(i_a)+\xi \tag{3}$$

where $u_{a0}(t)$ and $i_a(t)$ are the voltage and current of an arc having a constant length, L_0.

$$i_b(t)=\begin{cases} I_0 & \left|i_a(t)\right|<I_0 \\ \left|i_a(t)\right| & \left|i_a(t)\right|\geq I_0 \end{cases} \tag{4}$$

U_a, U_b, I_0 ($I_0\neq 0$), R_δ and ξ are all parameters defining the shape of the arc voltage. In (3), sgn is the sign function: sgn(x) = 1 if $x\geq 0$ and sgn(x) = -1 if $x<0$. $\xi(t)$ is zero-mean Gaussian noise. U_a is the product of the arc voltage gradient, E_a, and the length of the arc path, L_a, (the distance between the arc electrodes). The term $U_b I_0/i_b(t)$ represents the arc ignition voltage, and the term $R_\delta\left|i_b(t)\right|$ is a quasi-linear part determined by arc current, i_a. For simplicity, R_δ is called the *arc resistance*; it is, however, only part of the total arc resistance, which is mainly determined by the value of U_a.

The arc model (3) does not consider the elongation of the arc; this can be achieved by multiplying (3) with a suitable elongation function, $L(t)$. As the elongation of an arc is random and non-linear, it is difficult to model exactly; however, for the laboratory arc, the initial arc length is known to be the distance between the two arc electrodes, L_0. The elongation function $L(t)$ can then be expressed as:

$$L(t)=L_0\left(1+\Delta L(t-T_i)\mathrm{h}(t-T_i)\right) \tag{5}$$

where $\Delta L(t-T_i)$ represents the arc elongation, T_i is the arc inception time, and h(t) is the Heaviside function.

In its simplest form, in (5) $\Delta L(t-T_i)$ can be selected as the rate of change of the arc length:

$$\Delta L(t)=\frac{1}{L_0}\frac{\mathrm{d}L}{\mathrm{d}t}(t-T_i)\mathrm{h}(t-T_i) \tag{6}$$

Then, by combining (5) and (6), $L(t)$ becomes:

$$L(t)=L_0\left[1+\frac{1}{L_0}\frac{\mathrm{d}L}{\mathrm{d}t}(t-T_i)\mathrm{h}(t-T_i)\right] \tag{7}$$

$\Delta L(t-T_i)$ can be extended to a polynomial of the N^{th} degree with variable t.

For this paper, an exponential function was selected for the elongation function:

$$L(t)=L_0\left[1+A\mathrm{e}^{B(t-T_i)}\,\mathrm{h}(t-T_i)\right] \tag{8}$$

where A and B are parameters determining the arc elongation dynamics and:

$$\Delta L(t-T_i)=A\mathrm{e}^{B(t-T_i)}\,\mathrm{h}(t-T_i). \tag{9}$$

Therefore, by combining all of the above expressions, the new arc model can be expressed as:

$$\begin{aligned} u_a(t)&=u_{a0}(t)L(t-T_i)\mathrm{h}(t-T_i)= \\ &=u_{a0}(t)L_0\left[1+\Delta L(t-T_i)\mathrm{h}(t-T_i)\right] \end{aligned} \tag{10}$$

The term L_0 must be used in (3), otherwise voltage gradients E_a and E_b should be used instead of voltages U_a and U_b. It then follows that:

$$u_a(t)=u_{a0}(t)\left[1+\Delta L(t-T_i)\mathrm{h}(t-T_i)\right] \tag{11}$$

Then, by combining (9) and (11), we get:

$$u_a(t)=u_{a0}(t)\left[1+A\mathrm{e}^{B(t-T_i)}\,\mathrm{h}(t-T_i)\right] \tag{12}$$

The values for A and B depend on the specific case analysed and can be determined by the classical curve fitting methods.

The elongation effects from equation (12) introduce dynamic behaviour into the purely static model (3), so the final model is a *quasi-dynamic* arc model.

B. EMTP Simulation

The arc model has been implemented within the ATP-EMTP environment by making use of the Models interface tool. The new arc model requires the fault current for each time instant as an input parameter. By applying (3), (4) and (12) the arc voltage is computed, and the arc resistance is calculated by dividing the arc voltage with the fault current. In this way, the arc resistance is provided at each time step. It is exported from Models to ATP-EMTP by the type-91 variable resistance. In Fig. 4 the representation of the arc modelling in ATP-EMTP is shown.

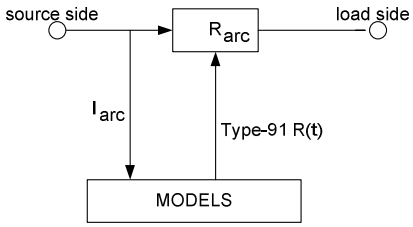

Fig.4 Representation of the arc model in ATP-EMTP

The laboratory test circuit shown was simulated using the ATP-EMTP software package and the quasi-dynamic arc model. The circuit parameters were: $u(t)$ = 21kV RMS, R = 0.65Ω, L = 9.55mH. The arc model parameters were: U_a = 1.55kV, U_b = 1.6kV, R_δ = 0.1Ω, A = 0.45 and B = 5.25s^{-1}. The arc inception time was set to t_i = 0.056s.

The parameters of the arc model can be determined by processing real arc voltage and current records and by using different estimation methods, methods based on Artificial Intelligence, or optimisation techniques. Parameters A and B can be easily extracted from the asymptotic elongation offset. Parameters U_a, U_b and R_δ define the arc voltage shape between two current zero-crossings. U_a determines the magnitude of the rectangular part of the arc voltage waveform. This value can be determined as an average of the half-cycle of the arc voltage. The parameter U_b determines the ignition voltage, so that it should correspond to this value obtained from a real voltage record. The parameter R_δ determines the arc behaviour during peak values of the arc current.

In Fig. 5 the simulated line terminal voltage $u(t)$ is presented. There is some distortion caused to the voltage by the fault arc which grows as the arc length increases. The simulated arc voltage $u_a(t)$ and current $i_a(t)$, are shown in Fig. 6. As the arc length increases there is a corresponding increase in the arc resistance, leading to a slight decrease in the amplitude of the arc current. The simulated arc *u-i* characteristic is presented in Fig. 7, showing that the arc is non-linear and time-varying; the increase in the arc voltage due to the arc elongation is patent. Fig. 8 shows a comparison of the real and simulated arc voltages; it is obvious that the two waveforms are very similar. The *AirArc* model can be simulated with or without random noise added to the voltage waveform. If no random noise is added, the correlation coefficient between the real and simulated arc voltage waveforms is r = 0.9565. With random noise added, the correlation coefficient between the two waveforms is different each time the model is simulated as the random noise is different each time. The model was simulated times with random noise and the average correlation coefficient was found to be r = 0.9529. This proves that the arc model is realistic and suitable for modelling applications, both with or without random noise. Whilst it is possible to add random noise to the simulated arc, it is not possible to replicate exactly the random elongation of the recorded arc.

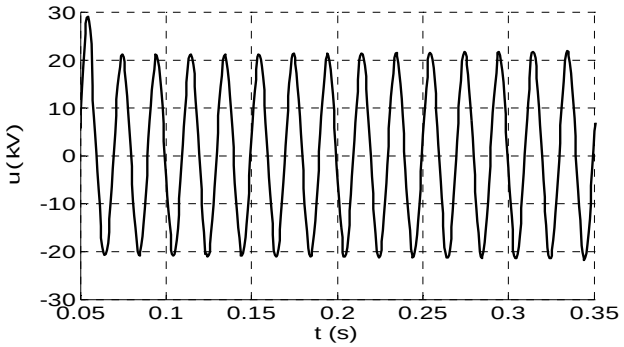

Fig. 5: Simulated line terminal voltage.

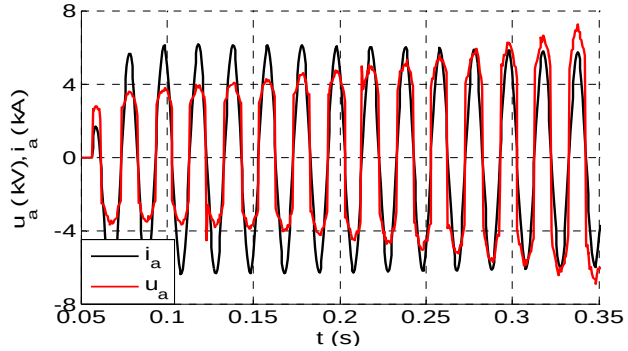

Fig. 6: Simulated arc voltage (red) and arc current (black).

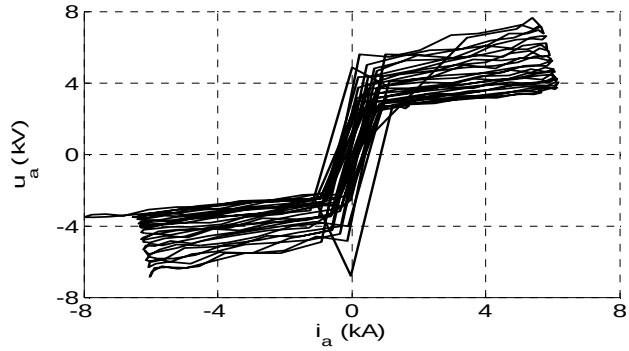

Fig. 7: Simulated arc *u-i* characteristic.

IV. Features of the Simulated Arc

In this Section the time domain and the spectral domain features of the arc simulated by using equation (12) are investigated.

A. *Time Domain Features*

The comparisons between the time-varying conductance, resistance and instantaneous power of the real arc and those from the simulated arc are presented in Figs 9, 10 and 11, respectively. The amplitudes of these features change with the arc elongation: the resistance and power increase over the arc's duration; the conductance decreases. It is obvious that in each case the arc model gives an accurate representation of the features of the real arc.

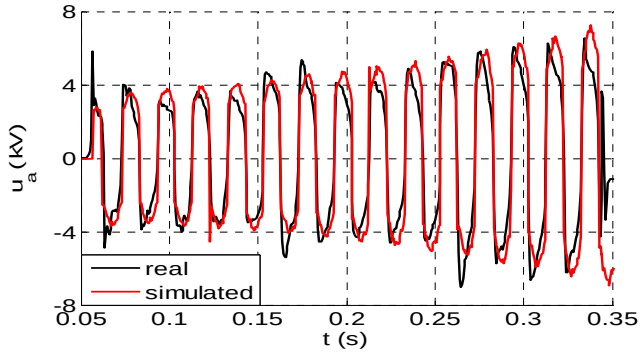

Fig. 8: Real (black) and simulated (red) arc voltages.

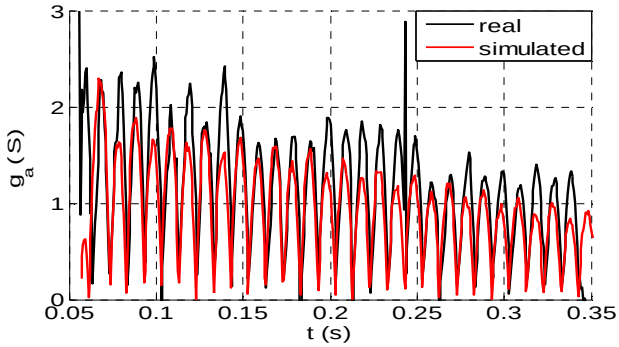

Fig. 9: Time-varying real (black) and simulated (red) arc conductance.

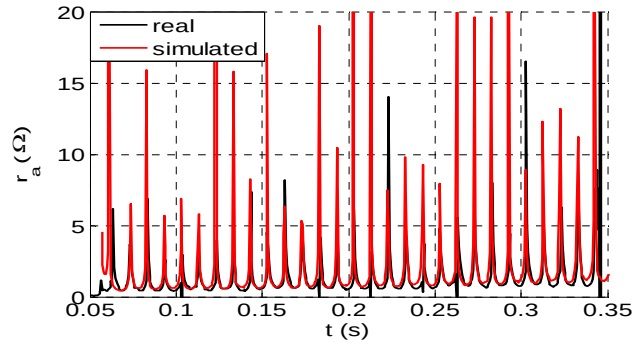

Fig. 10: Time-varying real (black) and simulated (red) arc resistance.

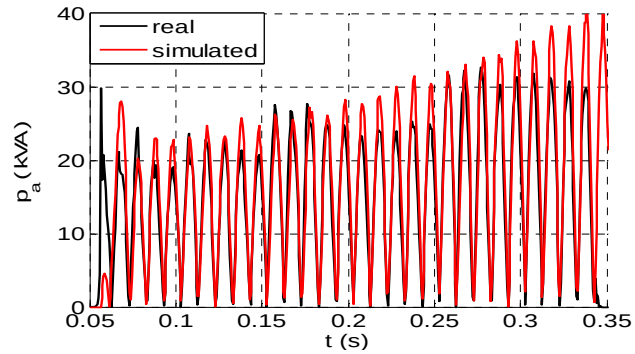

Fig. 11: Time-varying instantaneous real (black) and simulated (red) arc power.

B. Spectral Domain Features

Electrical fault arcs are known to be a significant source of harmonic distortion on power systems due to their distorted voltage waveforms. Therefore, for an arc model to be realistic in all aspects, it must also represent the spectral domain behaviour of real arcs accurately.

If only the first term of (3), U_a, is used and the random noise $\xi(t)$ is ignored, a purely rectangular (square) arc voltage waveform is obtained. A pure square wave has a Fourier series consisting of odd sin components only:

$$u_a(t) = \sum_{h=1}^{\infty} \frac{4}{\pi}\frac{1}{h} U_a \sin(h\omega t) \tag{13}$$

Where $h = 1, 3, 5, 7, \ldots$ is the harmonic order and ω is the fundamental angular frequency. Hence, the arc voltage harmonic spectrum contains only odd harmonics with amplitudes proportional to $1/h$. Therefore, the total harmonic distortion factor THD_{rec} of the arc voltage can be found as:

$$THD_{\text{rec}} = 100\sqrt{\sum_{h=2}^{M} \frac{1}{h^2}} \tag{14}$$

For THD_{rec} the following holds:

$$\lim_{h\to\infty} THD_{\text{rec}} = 100\sqrt{\pi^2/8 - 1} = 48.3\% \tag{15}$$

(Note that $\sum_{h=1}^{\infty} 1/h^2 = \pi^2/8$ if $h = 1, 3, 5, 7, \ldots$)

Here, the Fast Fourier Transform (FFT) was used to perform spectral analysis of the arc. The *THD* of the terminal voltage, the arc voltage and the arc current was then calculated. The results from the real arc and the simulated arc were obtained and compared in the graphs presented below.

Fig. 12 shows a comparison of the *THD* of the real and simulated test circuit terminal voltage. The *THD* of the simulated terminal voltage is smaller than that of the real terminal voltage due to the greater distortion in the real terminal voltage immediately after the fault inception time, but otherwise the THD of both voltages is very similar.

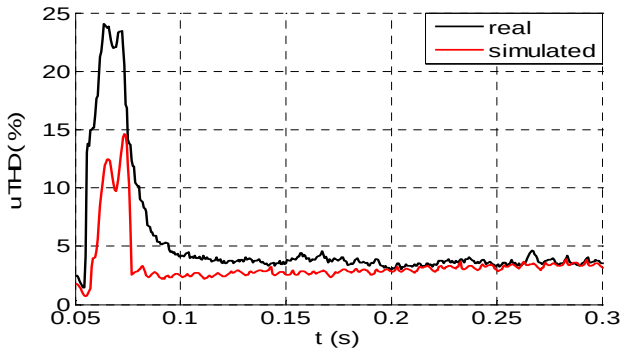

Fig. 12: Real (black) and simulated (red) terminal voltage THD.

The *THD* of the real and simulated arc voltage is presented in Fig. 13. Due to the random nature of the arc voltage, the *THD* of the real arc voltage does not reach a steady value; however, as the simulated arc voltage is of a similar shape to that of the real arc, the *THD* of the simulated arc is within the same range as the real arc. The difference in the level of *THD* in the real and simulated arc voltages shown in Fig. 13 can be attributed to the simulated arc being based on an equation that gives a rectangular waveform. As shown in (13), a rectangular waveform contains much more harmonic distortion than a sinusoidal waveform; thus, the simulated arc voltage contains more harmonic distortion than the real arc voltage waveform which has a more sinusoidal waveform.

Fig. 14 is a plot of the *THD* of the real and simulated arc current. The *THD* of the simulated arc current is slightly smaller than that of the real arc, but overall the two show good agreement.

As the *THD* of the simulated arc was found to be an accurate representation of that of the real arc in each of the cases above, the new quasi-dynamic arc model has been shown to accurately represent the spectral domain behaviour of a long arc in free air.

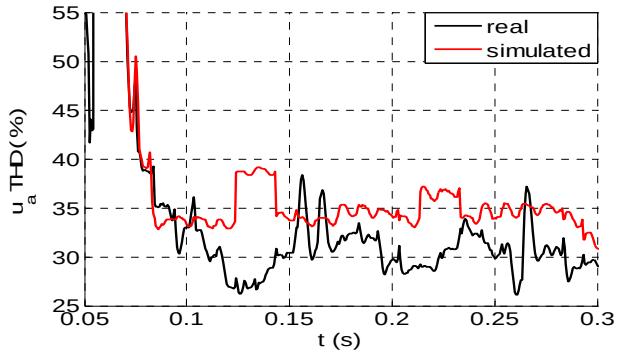

Fig. 13: Real (black) and simulated (red) arc voltage THD.

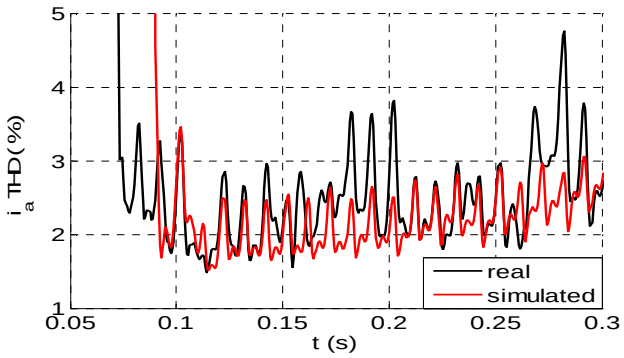

Fig. 14: Real (black) and simulated (red) arc current THD.

V. Conclusions

In this paper a new quasi-dynamic arc model that includes arc elongation and random noise was presented and incorporated into the EMTP software package. Data from a real laboratory was analysed and it was concluded that the arc grew randomly and non-linearly over its duration. As a result of this, the arc voltage and resistance also increase over time. The arc elongation effects were added to the presented arc model by means of an exponential function with parameters which can be determined using curve fitting methods. The random noise was added to the model by means of a random noise function in the Models interface in ATP-EMTP. The voltage waveform of the simulated arc was compared with that of the real arc, and it was found that the arc model was highly accurate, both with and without added random noise. It was also found that the time domain and spectral domain features of the simulated arc were very realistic. This means that the presented arc model is suitable for arcing fault simulation applications.

References

[1] A.M.Cassie, "Arc rupture and circuit severity, a new theory", CIGRE-Ber., Nr. 102, 1939

[2] O.Mayr, "Beiträge zur Theorie des statischen und dynamischen Lichtbogens, Arch. Elektrotechn., Bd. 37, pp.588-608, 1943

[3] J.Urbanek., "Zur Berechnung des Schaltverhaltens von Leistungsschaltern, eine erweiterte Mayr-Gleichung", ETZ-A, Bd. 93, H. 7, pp.381-385, 1972

[4] M.Kizilcay, T.Pniok. "Digital Simulation of Fault Arcs in Power Systems." ETEP Vol.1, No. 1, Jan/Feb 1991.

[5] A.T.Johns, R.K.Aggarwal, Y.H.Song. "Improved techniques for modelling fault arcs on faulted EHV transmission systems." IEE Proc.-Gener. Transm. Distrib., Vol.141, No.2, March 1994.

[6] V.Terzija, H.-J.Koglin, "On The Modeling of Long Arc in Still Air And Arc Resistance Calculation", IEEE Transactions on Power Delivery, Vol. 19, No. 3, July 2004, Page(s): 1012- 1017.

[7] M.Djurić, V.Terzija, "A new approach to the arcing faults detection for autoreclosure in transmission systems," *IEEE Trans. on Power Delivery*, Vol. 10, No 4, October 1995, pp. 1793-1798.

[8] Z.M.Radojević, V.V.Terzija, M.B.Djurić, "Multipurpose Overhead Lines Protection Algorithm", IEE Proc.-Gener.Transm Distrib., Vol. 146, No. 5, pp.441-445, September 1999.

[9] M.Djurić, Z.Radojević, V.Terzija, "Time Domain Solution Of Fault Distance Estimation And Arcing Faults Detection On Overhead Lines", IEEE Transactions on Power Delivery, Vol. 14, No. 1, January 1999, pp. 60 67

[10] User Support & Maintenance Centre Ontario Hydro "The Electromagnetic Transients Program (EMTP)", EMTP96 Version 3.1, Ontario Hydro, Nov. 1998.

[11] Alternative Transients Program (ATP) Rule Book.

[12] Manitoba HVDC Research Centre, "Powerful Transients Simulation Software PSCAD/EMTDC" Version 3.0.2, 1998.

[13] A.P.Strom, "Long 60-cycle Arc in Air", Trans. Am. Inst. Elec. Eng., 65, pp.113-117, 1946.

[14] Warrington, A.R.Van C., "Reactance Relays Negligibly Affected by Arc Impedance", Electrical World, September, 19, pp. 502-505, 1931.

[15] T.E.Browne, Jr., "The Electric Arc as a Circuit Element", Journal of Electrochem. Soc. Vol. 102 No. 1, pp. 27-37, 1955.

[16] A.S.Maikapar, "Extinction of an open electric arc," Elektrichestvo, Vol. 4, pp. 64-69, April 1960.

[17] A.Papoulis, *Probability, Random Variables and Stochastic Processes*, 3rd ed. New York: McGraw-Hill, 1991.

[18] V.Terzija, H.-J.Koglin, "Long Arc In Free Air: Testing, Modelling And Parameter Estimation: Part I", UPEC 2000 Conference, Belfast, UK, Sep. 2000.

[19] V.Terzija, H.-J.Koglin, "Long Arc In Free Air: Testing, Modelling And Parameter Estimation: Part II", UPEC 2000 Conference, Belfast, UK, Sep. 2000.